
Geological Survey of Canada
Commission géologique du Canada

PAPER 83-27

**CONTRIBUTIONS TO X-RAY
FLUORESCENCE SPECTROSCOPY**

PART I

**A COMPARISON BETWEEN THEORETICAL AND
EXPERIMENTAL CORRECTIONS FOR INTERFERING
SPECTRAL LINES FROM TARGET ELEMENTS IN
X-RAY FLUORESCENCE SPECTROSCOPY**

PART II

**COMPARISON OF X-RAY TUBES USED FOR MAJOR
AND TRACE ELEMENT ANALYSIS IN X-RAY
FLUORESCENCE SPECTROSCOPY**

**A.G. HEINRICH
A.E. FOSCOLOS**



PAPER 83-27

CONTRIBUTIONS TO X-RAY FLUORESCENCE SPECTROSCOPY

PART I

**A COMPARISON BETWEEN THEORETICAL AND
EXPERIMENTAL CORRECTIONS FOR INTERFERING
SPECTRAL LINES FROM TARGET ELEMENTS IN
X-RAY FLUORESCENCE SPECTROSCOPY**

PART II

**COMPARISON OF X-RAY TUBES USED FOR MAJOR
AND TRACE ELEMENT ANALYSIS IN X-RAY
FLUORESCENCE SPECTROSCOPY**

**A.G. HEINRICH
A.E. FOSCOLOS**

© Minister of Supply and Services Canada 1984

Available in Canada through

authorized bookstore agents and other bookstores

or by mail from

Canadian Government Publishing Centre
Supply and Services Canada
Ottawa, Canada K1A 0S9

and from

Geological Survey of Canada offices:

601 Booth Street
Ottawa, Canada K1A 0E8

3303-33rd Street N.W.,
Calgary, Alberta T2L 2A7

100 West Pender Street
Vancouver, British Columbia V6B 1R8
(mainly B.C. and Yukon)

A deposit copy of this publication is also available
for reference in public libraries across Canada

Cat. No. M44-83/27E
ISBN 0-660-11622-7

Canada: \$4.00
Other countries: \$4.80

Price subject to change without notice

Critical Readers

D. Morrow
J. Nicholls

Original manuscript received: 1982 - 05 - 28
Final version approved for publication: 1984 - 03 - 09

CONTENTS

CONTRIBUTIONS TO X-RAY FLUORESCENCE SPECTROSCOPY

PART I

A COMPARISON BETWEEN THEORETICAL AND EXPERIMENTAL CORRECTIONS FOR INTERFERING SPECTRAL LINES FROM TARGET ELEMENTS IN X-RAY FLUORESCENCE SPECTROSCOPY

1	Abstract/Résumé
1	Introduction
4	Sample preparation and operating conditions
10	Experimental method and results
10	Determination of trace element concentrations by calculating and eliminating the effects of interfering spectral lines from targets, on samples of known chemical composition
10	Determination of trace element concentrations by calculating and eliminating the effects of interfering spectral lines from targets, on samples of unknown chemical composition
10	Discussion
11	References
12	Appendix: Calculations for Cu and Zn concentrations in W-1 standard rock samples

Illustrations

Figures

2	1. Intensity of $\text{CuK}\alpha$ spectral line vs. mass absorption
2	2. Intensity of $\text{ZnK}\alpha$ spectral line vs. mass absorption
2	3. Intensity of $\text{PbL}\alpha$ spectral line vs. mass absorption
3	4. Mass absorption vs. intensity of Rh Compton line
3	5. Mass absorption of $\text{CuK}\alpha$ vs. mass absorption of Rh Compton line
3	6. Mass absorption of $\text{ZnK}\alpha$ vs. mass absorption of Rh Compton line
4	7. Mass absorption of $\text{PbL}\alpha$ vs. mass absorption of Rh Compton line

Tables

4	1. Calculated mass absorption coefficients and measured intensities of $\text{RhK}\alpha$ scatter (Compton) line of different materials
5	2. Operating conditions for Philips X-ray Fluorescence Spectrometer PW1212 with 2kW rated generator, using Cu, Zn and Pb
5	3. Trace element analysis of Cu and Zn in W-1 standard sample
6	4. Ratios of mass absorption coefficients of various materials at different wavelengths
6	5. Determination of Cu and Zn in W-1 sample, using AGV-1 as a standard
7	6. Comparison of different values for Cu, Zn and Pb content derived from various analytical methods
8-9	7. Calculation of coherent scattering (S_{coh}) for λCu
8-9	8. Calculation of coherent scattering (S_{coh}) for λZn

CONTENTS (cont'd.)

PART II

COMPARISON OF X-RAY TUBES USED FOR MAJOR AND TRACE ELEMENT ANALYSIS IN X-RAY FLUORESCENCE SPECTROSCOPY

13	Abstract/Résumé
13	Introduction
14	Materials and methods
14	Results
16	Discussion
16	Conclusion
18	Acknowledgments
18	References

Illustrations

Figures

15	1. Relative intensity of Rh/Cr vs. atomic number
15	2. Relative intensity of Mo/Cr vs. atomic number
15	3. Relative intensity of W/Cr vs. atomic number
15	4. Spectrum intensity of Cr vs. wavelength
15	5. Spectrum intensity of Rh vs. wavelength
16	6. Spectrum intensity of Mo vs. wavelength
16	7. Spectrum intensity of W vs. wavelength
17	8. Illustration of tube spectrum and analyte spectrum

Tables

14	1. Operating conditions
18	2. Comparison of detection limits
18	3. Optimum tubes for elements analyzed

PART I

A COMPARISON BETWEEN THEORETICAL AND EXPERIMENTAL CORRECTIONS FOR INTERFERING SPECTRAL LINES FROM TARGET ELEMENTS IN X-RAY FLUORESCENCE SPECTROSCOPY

Abstract

Trace element analysis by X-ray fluorescence spectroscopy of rocks, soils, minerals, coals and coal ashes can yield erroneous results for elements which also occur as impurities in targets. Spectral lines originating from the target impurities add intensity to the spectral lines originating from the samples being analysed. However, the increase is not constant and depends upon the mass absorption coefficient of the sample. The problem is critical when small concentrations are to be determined.

Earlier methods used in correcting for interfering spectral lines from targets have required the prior knowledge of the major chemical constituents of the materials being analyzed in order to calculate the mass absorption coefficients. The purpose of this paper is to present alternative, more rapid but equally accurate methods for establishing mass absorption coefficients without requiring prior knowledge of the major constituents. This requirement has been a drawback when large numbers of geological samples were being analysed. Test results are also compared with results calculated theoretically.

Résumé

L'analyse des éléments traces par la spectrographie fluorescente à rayons X des échantillons de roches, de sols, de minéraux, de charbons et de cendres de charbon peut donner des résultats erronés pour des éléments contaminants cibles. Des lignes spectrales qui proviennent des contaminants cibles augmentent l'intensité des lignes spectrales qui proviennent des échantillons destinés à l'analyse. Cependant, l'augmentation n'est pas constante et dépend du coefficient d'absorption massique de l'échantillon. Le problème critique se pose lorsqu'il s'agit d'analyser de petites concentrations.

Des méthodes plus anciennes utilisées pour minimiser l'interférence des lignes spectrales provenant de contaminants exigeaient une connaissance préalable de composants majeurs des matériaux analysés, afin de calculer les coefficients d'absorption massique. Le but de cette étude est de présenter des méthodes rapides, mais tout aussi efficaces, pour calculer les coefficients d'absorption massique sans, toutefois, connaître au préalable, les constituants majeurs. Jusqu'à maintenant un tel besoin a été un inconvénient au moment où on devait analyser de nombreux échantillons. Des résultats d'analyse sont comparés aux résultats théoriques.

Introduction

The use of filters to remove interfering spectral lines originating from target elements has been proposed by Jenkins and De Vries (1969). However, the lack of available and suitable filter materials for some spectral lines, and the difficulties encountered in preparing filters with correct thickness, render the filtering technique inadequate.

The theoretical basis for correcting the effect of interfering spectral lines from target elements is discussed by Steele (1973). It involves two equations, which are presented in the appendix along with other calculations pertinent to the subject of this paper. These two equations presuppose a knowledge of the major elemental rock composition prior to the determination of the concentration of trace elements. In the past, a prior knowledge of the major elemental composition of the sample has been necessary, in order to calculate the intensity of the interfering spectral lines of the tube, as this affects the concentration measurements.

In the present work, the use of two different approaches to overcome the problem of interfering spectral lines from the target are discussed, based upon the combined work of Hower (1959), Reynolds (1963), Schröhl and Štepan (1969), Franzini et al. (1976), and Sumartojo and Paris (1980).

One approach, like Steele's (1973), is based upon the prior knowledge of the major elemental composition of the rock, soil, or coal ash sample, while the other does not require this advance information. The latter method is suitable for routine analysis of geological material. A comparative study between theoretical and experimental corrections for interfering spectral lines from a Rh target has shown that the alternative technique proposed in this paper is simpler, faster and yields good results, comparable in quality to those achieved using Steele's method.

The correction required for the interfering spectral lines of specific tubes must be determined individually by users in their own laboratories, as elemental contaminants vary from tube to tube, both in type and amount.

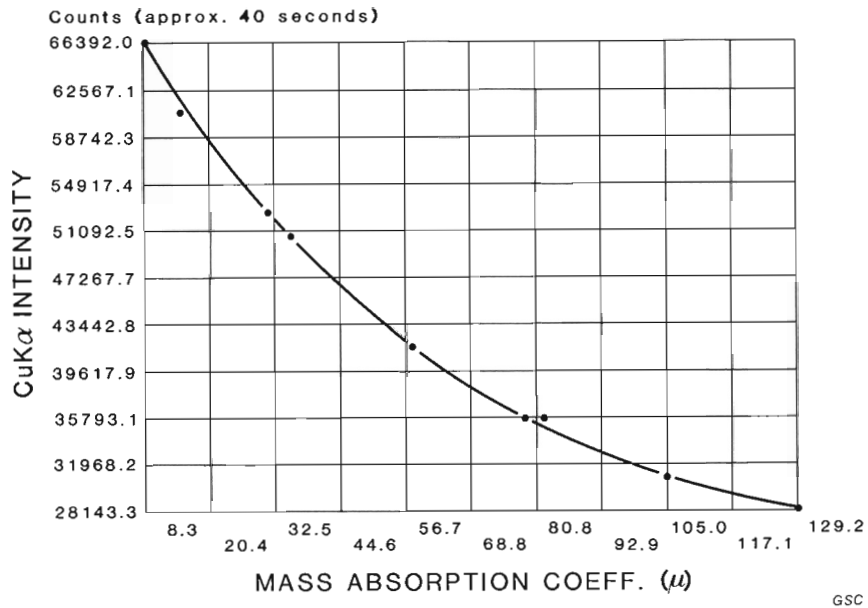


Figure 1. Intensity of CuK α spectral line vs. mass absorption. Note: CuK α (λ) = 1.542Å.

Figure 2. Intensity of ZnK α spectral line vs. mass absorption. Note: ZnK α (λ) = 1.436Å.

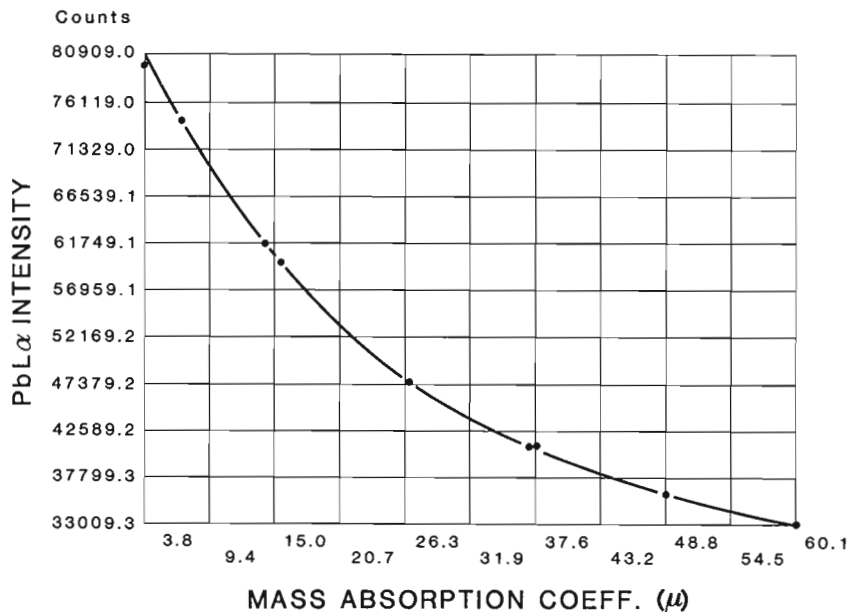
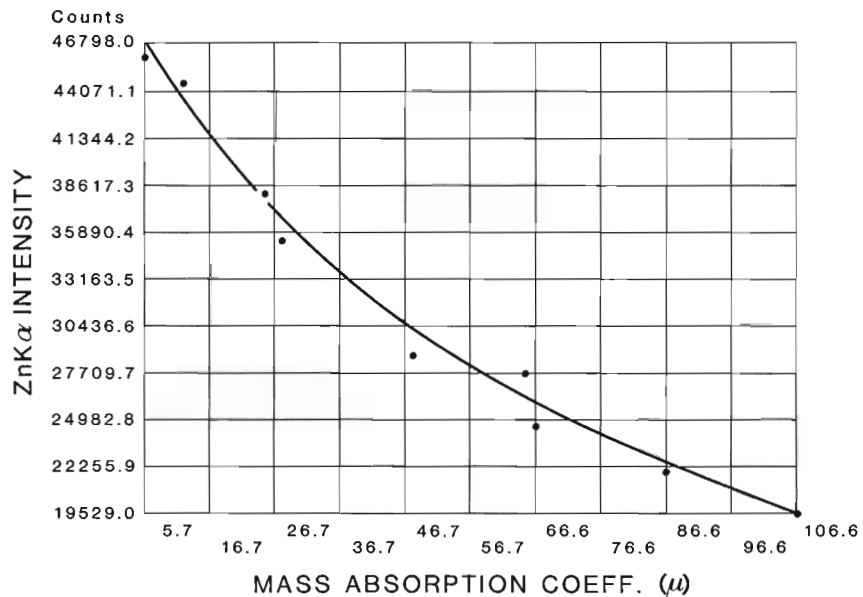


Figure 3. Intensity of PbL α spectral line vs. mass absorption. Note: PbL α (λ) = 1.175Å.

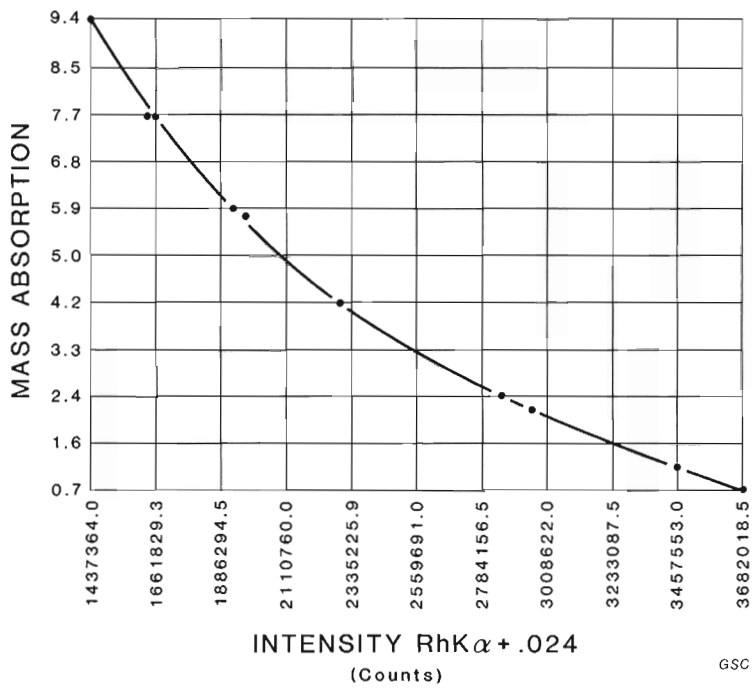


Figure 4. Mass absorption vs. intensity of Rh Compton line.

Figure 5. Mass absorption of CuKα vs. mass absorption of Rh Compton line.

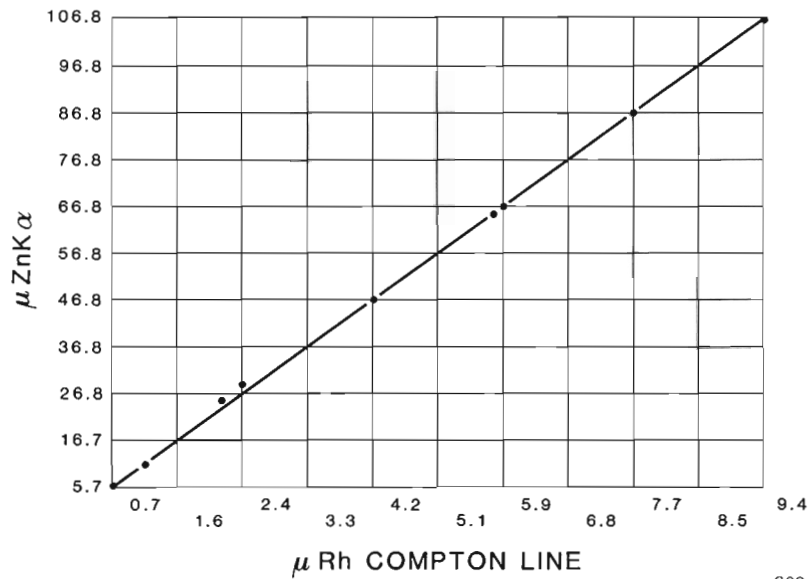
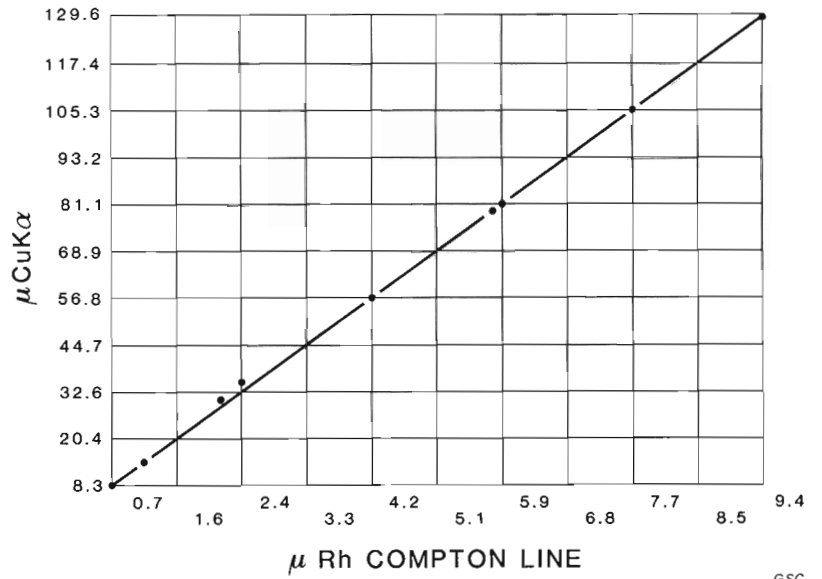


Figure 6. Mass absorption of ZnKα vs. mass absorption of Rh Compton line.

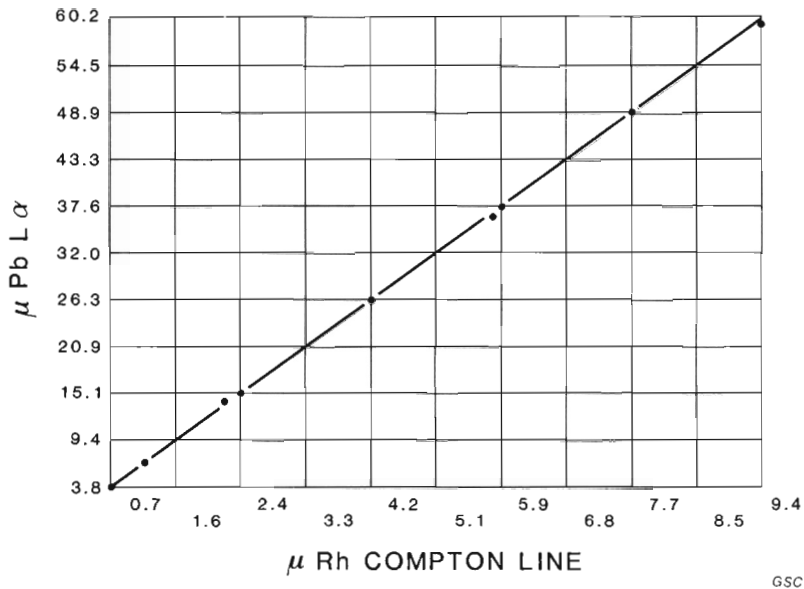


Figure 7. Mass absorption of PbL α vs. mass absorption of Rh Compton line.

Table 1

Calculated mass absorption coefficients* and measured intensities of RhK α scatter (Compton) line of different materials

Materials	Designation of Materials	Intensities of RhK α Compton Scatter 0.615 + 0.0243	Wavelength					
			0.615 + 0.0243 RhK α	2.103 MnK α	1.937 FeK α	1.542 CuK α	1.436 ZnK α	1.175 PbL α
Li ₂ B ₄ O ₇	1TC	3,682,017	0.71	20.18	15.68	8.31	6.74	3.77
Li ₂ B ₄ O ₇ /SiO ₂ (0.75/0.25)	2TC	3,459,837	1.17	35.99	28.33	14.98	12.20	6.79
Al ₂ O ₃	3TC	2,973,741	2.27	75.34	60.41	31.13	25.62	14.22
SiO ₂	4TC	2,859,111	2.53	83.45	66.29	35.01	28.56	15.86
SiO ₂ /CaO (0.75/0.25)	5TC	2,297,838	4.25	136.20	106.54	58.56	48.06	26.92
Al ₂ O ₃ /CaO (0.50/0.50)	6TC	1,969,667	5.84	184.90	143.84	80.17	66.09	37.16
SiO ₂ /CaO (0.50/0.50)	7TC	1,924,850	5.97	188.95	146.78	82.11	67.56	37.97
SiO ₂ /CaO (0.25/0.50)	8TC	1,656,081	7.68	241.71	187.02	105.66	87.07	49.03
CaO	9TC	1,437,364	9.40	294.46	227.27	129.21	106.57	60.09
AGV-1	AGV-1	2,327,864	4.06	97.79	89.19	54.29	44.80	25.44
W-1	W-1	2,110,546	5.02	106.76	84.25	66.43	54.99	31.44

*Preset counts of 1,000,000 in normalizer; Rh tube 60kV - 32 mA, LiF crystal, fine collimator, and flow and scintillation counter.

It should be emphasized that, although the present work is based on a limited number of samples, later investigations have supported the validity of the results, and the main intent of this paper is to demonstrate the technique, the application of the methods, and the step-by-step calculation involved.

Sample preparation and operating conditions

In order to study the influence of the mass absorption coefficient, μ , on the intensity of the interfering spectral lines for the tube, Li₂B₄O₇, Al₂O₃, SiO₂ and CaO compounds were used, either pure, or as mixtures of two. The proportions and the calculated mass absorption coefficients are presented in Table 1. The compounds were fused in order

to prepare a glass bead. This mixture consisted of 1.000 g of sample, 1.00 g of oxidant (NH₄NO₃), and 5.30 g of flux. The flux consisted of 5.00 g of Li₂B₄O₇ and 0.30 g of LiF. The mixture was fused at 1000°C using Claisse Fluxer apparatus. The advantages of having fused beads are: a homogeneous sample, elimination of mineral and grain size effects, minimum inter-elemental effects, and common oxide form for every element. The disadvantage of having a slight drop in intensity is counterbalanced by the advantages.

The operational conditions for the P.W. 1212 Philips X-ray Fluorescence Spectrometer, 2 kW rated generator, are presented in Table 2.

Table 2

Operating conditions for Philips X-ray Fluorescence Spectrometer PW1212 with 2kW rated generator, using Cu, Zn and Pb.

Tube and Power: Rh tube, 60 kV, 32mA

Crystal: LiF 200

Angle of Incidence: 55°

Collimator: 150 μm

Take off Angle: 35°

Radiation Path: Vacuum

Counter: Scintillation counter 1050 volts + Flow counter 1750 volts

Measuring Time: Fixed counts for normalizer = 30,000 counts, and for RhKα = 10⁶ counts

ELEMENT	Rh	Cu	Zn	Pb
Analytical Line	Kα (Scatter)	Kα	Kα	Lα
Peak 2θ Angle	18.40	45.11	41.88	34.07
Background 2θ Angle	-	43.50	43.50	34.80
Background Factor	-	.8846	1.1458	1.1566
Normalizer	A-139-1*	A-139-1	A-139-1	A-139-1

*Elemental Composition: 67.36% SiO₂, 16.22% Al₂O₃, 3.52% Fe₂O₃, 3.00% CaO, 1.02% MgO, 2.79% K₂O, 3.39% Na₂O, 5,000 ppm TiO₂, 800 ppm MnO, 200 ppm Cu, 200 ppm Ni, 200 ppm Pb and 200 ppm Zn.

Table 3

Trace element analysis of Cu and Zn in W-1 sample using AGV-1 rock sample as a reference with reported concentrations, (Abbey, 1980) of 59 ppm Cu and 86 ppm Zn.

Samples	μ Cu	Total Counts	Counts from Target Interference	Net Counts
AGV-1	54.29	47,689	43,138	4,551
W-1	66.43	46,792	39,433	7,359

$$C_{un} = C_{st} \times \frac{I_{un}}{I_{st}} \times \frac{\mu_{un}}{\mu_{st}} = 59 \times \frac{7359}{4551} \times \frac{66.43}{54.29} = 117 \text{ ppm Cu}$$

Samples	μ Zn	Total Counts	Counts from Target Interference	Net Counts
AGV-1	44.80	36,326	30,938	5,388
W-1	54.99	37,727	28,306	4,421

$$C_{un} = C_{st} \times \frac{I_{un}}{I_{st}} \times \frac{\mu_{un}}{\mu_{st}} = 86 \times \frac{4421}{5381} \times \frac{54.99}{44.80} = 87 \text{ ppm Zn}$$

A normalizer was used to counterbalance instrument instability, humidity conditions, and crystal drift, which occur from day to day. The normalizer is composed of common minerals, such as feldspars, quartz, and ilmenite, and pure compounds such as CuSO₄. The chemical composition of the normalizer, A-139-1, is presented in Table 2. The precise composition of the normalizer is not required, since reliable statistics can be obtained if a sufficient number of counts is made for each element being analysed. Phenol formaldehyde was used to bind the materials together and help preserve the pellet for a long period of time. The ratio of phenol formaldehyde to sample is 4:1. The number of counts considered sufficient varies from element to element --- for example, rates of about 500 cps for sodium and 20,000 cps for iron are required. The count should be accomplished within a reasonable time frame of one or two minutes.

The correction of interfering spectral lines concerns only those elements with wavelength λ less than the K absorption edge of Fe. For example, the correction can be made for Cu but not for Ca.

For the purpose of this work, sample W-1 was treated as the unknown and sample AGV-1 as the reference standard. Both W-1 and AGV-1 are certified reference standard samples of silicate rocks and can be obtained from the United States Geological Survey.

Table 4

Ratios of mass absorption coefficients of various materials at different wavelengths

Designation of Materials	Wavelength					
	.639	2.103	1.937	1.542	1.436	1.175
1TC/2TC	.607	.561	.553	.555	.552	.555
2TC/3TC	.515	.478	.469	.481	.476	.477
3TC/4TC	.897	.903	.911	.889	.897	.897
4TC/5TC	.595	.613	.622	.598	.594	.589
5TC/6TC	.728	.737	.741	.730	.727	.724
6TC/7TC	.978	.979	.980	.976	.978	.979
7TC/8TC	.777	.782	.785	.777	.776	.774
8TC/9TC	.817	.821	.823	.818	.817	.816
1TC/9TC	.076	.069	.069	.064	.063	.063
AGV-1/W-1	.809	.916	1.059	.817	.815	.809

Table 5

Determination of Cu and Zn in W-1 sample, using AGV-1 as a standard

(Note: The Intensities of the Compton RhK α , CuK α , and ZnK α lines are taken from figures 1, 2, 4, 5, and 6)

Sample	Intensity of Compton RhK α Line	μ RhK α from Fig. 4	μ CuK α from Fig. 5	Total Intensity of CuK α Line	Intensity of Interfering CuK α Line from Fig. 1	Net Intensity (Counts)	Calculated Cu Value in ppm	Reported Cu Value in ppm	Per cent Variation
AGV-1	2,327,860	4.14	56.63	47,689	42,363	5,326	110	110	0.0
W-1	2,110,550	5.05	69.25	46,792	38,678	8,114			

Sample	Intensity of Compton RhK α Line	μ RhK α from Fig. 4	μ ZnK α from Fig. 6	Total Intensity of ZnK α Line	Intensity of Interfering ZnK α Line from Fig. 2	Net Intensity (Counts)	Calculated Zn Value in ppm	Reported Zn Value in ppm	Per cent Variation
AGV-1	2,327,860	4.14	46.55	36,326	30,443	5,883	87	86	1.2
W-1	2,110,550	5.05	56.97	32,727	27,853	4,874			

Table 6

Comparison of different values for Cu, Zn and Pb content derived from various analytical methods

Sample	Compton RhK α	Intensity (Counts) of λ CuK α	Calculated μ CuK α	μ RhK α from Fig. 4	μ CuK α from Fig. 5	Interference (Counts) for CuK α	Net Counts	Calculated Cu Concentration in ppm	Reported Cu Concentration in ppm	Per cent Variation	Method used
AGV-1 (std.)	2,327,860	47,689				41,859	5,830	113	59	2.73	Steele's (1973) equation (see appendix)
W-1	2,110,550	46,792				37,705	9,087		110		
AGV-1 (std.)			54.29			43,138	4,551			6.36	Chemistry known; Fig. 1
W-1			66.43	4.14	56.63	39,433	7,359	117			
AGV-1 (std.)				5.05	69.25	42,363	5,326	110		0.00	Chemistry unknown; Figs. 1, 4, 5
W-1						38,678	8,114				
SiO ₂	2,859,111	18,375	35.01								
Sample	Compton RhK α	Intensity (Counts) of λ ZnK α	Calculated μ ZnK α	μ RhK α from Fig. 4	μ ZnK α from Fig. 6	Interference (Counts) for ZnK α	Net Counts	Calculated Zn Concentration in ppm	Reported Zn Concentration in ppm	Per cent Variation	Method used
AGV-1 (std.)	2,237,860	36,326				29,093	7,233	91	86	5.81	Steele's (1973) equation (see appendix)
W-1	2,110,550	37,727				26,462	6,265		86		
AGV-1 (std.)			44.80			30,938	5,388			1.16	Chemistry known; Fig. 2
W-1			54.99	4.14	46.55	28,306	4,421	87			
AGV-1				5.05	56.97	30,443	5,883	87		1.16	Chemistry unknown; Figs. 2, 4, 6
W-1						27,853	4,874				
SiO ₂	2,859,111	7,546	28.56								
Sample	Compton PbK α	Intensity (Counts) of λ PbL α	Calculated μ PbL α	μ RhK α from Fig. 4	μ PbL α from Fig. 7	Interference (Counts) for PbL α	Net Counts	Calculated Pb Concentration in ppm	Reported Pb Concentration in ppm	Per cent Variation	Method used
AGV-1 (std.)	2,327,860	57,053				48,498	8,555	31	33	?	Steele's (1973) equation (see appendix)
W-1	2,110,550	50,196				43,702	6,494		8		
AGV-1 (std.)			25.44			49,473	7,580			?	Chemistry known; Fig. 3
W-1			31.44	4.14	26.14	44,844	5,352	29			
AGV-1 (std.)				5.05	32.03	48,863	8,190	28		?	Chemistry unknown; Figs. 3, 4, 7
W-1						44,456	5,740				
SiO ₂	2,859,111	135	15.86								

Table 7

Calculation of coherent scattering (S_{coh}) for λ_{Cu} (where $\lambda_{Cu} = 1.5405$ radiation and take off angle of 35° . $S_x = \sin\theta/\lambda = \sin 35/1.5405 = 0.3719$)

Elements	Per cent in AGV-1	Per cent in W-1	Per cent in SiO ₂	Per cent in CaO	Per cent in Al ₂ O ₃	Per cent in Li ₂ B ₄ O ₇	S.F.*	F ²	Atomic weight A _i	C _i F _i ² /A _i for AGV-1
Si	27.87	24.64	46.75				7.59	57.61	28.08	57.18
Al	9.06	7.92			52.92		7.20	51.84	26.98	17.41
Fe	4.74	7.77					14.98	224.40	55.85	19.04
Ti	0.64	0.64					11.77	38.53	47.90	1.85
Mg	0.92	4.00					6.71	45.02	24.31	1.70
Ca	3.53	7.85		71.47			10.43	108.78	40.08	9.58
Na	3.20	1.59					5.40	29.16	22.99	4.06
K	2.42	0.53					9.78	95.65	39.10	5.92
O	45.92	45.35	53.25	28.53	47.08	66.22	3.45	11.90	16.00	34.15
Li						8.21	1.39	1.93	6.94	
B						25.57	1.79	3.20	10.81	
Total	98.30	100.29	100.00	100.00	100.00	100.00				
$\Sigma C_i F_i^2 / A_i$										150.89
$\Sigma C_i \mu_i$										
S_{coh}										0.0279

S.F.* = scattering factor computed for $S_x = 0.3720$ from tables, Cromer and Waber (1964)
See Appendix for definition of symbols.

Table 8

Calculation of coherent scattering (S_{coh}) for λ_{Zn} (where $\lambda_{Zn} = 1.659$ radiation and take off angle of 35° . $S_x = \sin\theta/\lambda = \sin 35/1.659 = 0.3460$)

Elements	Per cent in AGV-1	Per cent in W-1	Per cent in SiO ₂	Per cent in CaO	Per cent in Al ₂ O ₃	Per cent in Li ₂ B ₄ O ₇	S.F.*	F ²	Atomic weight A _i	C _i F _i ² /A _i for AGV-1
Si	27.87	24.64	46.75				7.79	60.68	28.08	60.23
Al	9.06	7.92			52.92		7.42	55.06	26.98	18.49
Fe	4.74	7.77					15.54	241.49	55.85	20.53
Ti	0.64	0.64					12.21	149.08	47.90	1.99
Mg	0.92	4.00					6.95	48.30	24.31	1.82
Ca	3.53	7.85		71.47			10.82	117.07	40.08	10.31
Na	3.20	1.59					6.34	40.20	22.99	6.16
K	2.42	0.53					10.14	102.82	39.10	6.36
O	45.92	45.35	53.25	28.53	47.08	66.22	3.65	13.32	16.00	38.23
Li						8.21	1.42	2.02	6.94	
B						25.57	1.84	3.39	10.81	
Total	98.30	100.29	100.00	100.00	100.00	100.00				
$\Sigma C_i F_i^2 / A_i$										164.12
$\Sigma C_i \mu_i$										
S_{coh}										0.0368

S.F.* = scattering factor computed for $S_x = 0.3460$ from tables, Cromer and Waber (1964)
See Appendix for definition of symbols.

Table 7 (cont'd)

$C_i\mu_i$ for AGV-1	$C_iF_i^2/A_i$ for W-1	$C_i\mu_i$ for W-1	$C_iF_i^2/A_i$ for SiO ₂	$C_i\mu_i$ for SiO ₂	$C_iF_i^2/A_i$ for CaO	$C_i\mu_i$ for CaO	$C_iF_i^2/A_i$ for Al ₂ O ₃	$C_i\mu_i$ for Al ₂ O ₃	$C_iF_i^2/A_i$ for Li ₂ B ₄ O ₇	$C_i\mu_i$ for Li ₂ B ₄ O ₇
1,772.37 440.32 1,467.50 129.28 36.25 621.99 94.08 359.13 528.08	50.55 15.22 31.23 1.85 7.41 21.31 2.02 1.30 33.73	1,522.75 384.91 240.54 129.28 157.60 1,383.17 46.74 78.65 521.53	95.91	2,889.15			101.68	2,572.40		
					193.97	12,593.00				
			39.60	612.38	21.22	328.10	35.02	541.39	49.25 2.28 7.57	761.53 5.76 63.41
	164.62		135.51		215.19		136.70		59.10	
5,449.00		4,465.17		3,501.53		12,921.10		3,113.79		830.70
	0.0248		0.0387		0.0167		0.0439		0.0711	

Table 8 (cont'd)

$C_i\mu_i$ for AGV-1	$C_iF_i^2/A_i$ for W-1	$C_i\mu_i$ for W-1	$C_iF_i^2/A_i$ for SiO ₂	$C_i\mu_i$ for SiO ₂	$C_iF_i^2/A_i$ for CaO	$C_i\mu_i$ for CaO	$C_iF_i^2/A_i$ for Al ₂ O ₃	$C_i\mu_i$ for Al ₂ O ₃	$C_iF_i^2/A_i$ for Li ₂ B ₄ O ₇	$C_i\mu_i$ for Li ₂ B ₄ O ₇
1,407.43 363.53 1,232.16 112.03 29.85 513.26 76.00 294.51 426.94	53.24 16.17 33.61 1.99 7.95 22.93 2.78 1.40 37.75	1,244.32 317.79 2,019.81 112.03 129.80 1,141.39 37.76 64.50 421.60	101.02	2,360.87			107.96	3,062.46		
					208.75	10,391.70				
			44.33	495.09	23.75	265.26	39.19	657.57	55.13 2.39 8.02	615.18 5.02 53.76
	177.82		145.35		232.50		147.15		65.54	
4,455.71		5,489.00		2,855.96		10,656.96		3,720.03		673.96
	0.0324		0.0509		0.0218		0.0396		0.0972	

Experimental method and results

Determination of trace element concentrations by calculating and eliminating the effect of interfering spectral lines from targets, on samples of known chemical composition

If the composition of the major elements in geological samples is known, the intensity of the interfering spectral lines from the target can be calculated. Using mixtures of various pure materials to obtain variable mass absorption coefficients, a graph can be derived of the intensity (counts) of interfering spectral lines from the target, as a function of the mass absorption coefficient for each interfering element. Figures 1, 2 and 3 indicate such a relationship. Table 3 outlines the calculation of Cu and Zn concentrations in sample W-1. The Cu and Zn concentrations of sample W-1 were considered unknown for the purpose of the test. The reported values (Abbey, 1980; Flanagan, 1969), for Cu and Zn in sample W-1 are 110 ppm and 86 ppm respectively, while the measured values for this test are 117 ppm and 87 ppm, a variation of 6.4 per cent and 1.2 per cent. The accuracy of the method is as good as the usable values of the standards.

Determination of trace element concentrations by calculating and eliminating the effects of interfering spectral lines from targets, on samples of unknown chemical composition

When the elemental composition of the sample is unknown the use of a graph is necessary. Figure 4 relates graphically the intensity of the incoherent scattering (Compton¹) line of the target (RhK α) to the various mass absorption coefficients (μ) of pure materials. The composition of the materials, their μ values, and the counts are presented in Table 1. The method of calculating μ was proposed by Reynolds (1963) and Sumartojo and Paris (1980). The coherent scatter line (Rayleigh line), as applied by Schröil and Stepán (1969) and Steele (1973), was not used in this experiment.

The mass absorption coefficient of the sample, obtained from the intensity of the Compton RhK α line, can be used to obtain the mass absorption coefficient of the same sample for any wavelength, λ , which is less than the K absorption edge of Fe. As a result, the mass absorption coefficient of the sample, obtained from the intensity of the Compton line of the Rhodium tube, can be used to obtain the mass absorption coefficient of the same sample for any wavelength which is less than the K absorption edge of Fe (Franzini et al., 1976; Sumartojo and Paris, 1980; Schröil and Stepán, 1969). The theoretical basis for this conversion is presented in Table 4. This table indicates that the ratio of the mass absorption coefficient at various wavelengths is constant. The ratios are obtained from Table 1. As a result, figures 5, 6 and 7 can be constructed. Figure 5 relates the mass absorption coefficient, obtained from the Compton K α line of the Rh target, to the mass absorption coefficient for CuK α . Table 5 makes use of figures 4, 5 and 6 for the samples AGV-1 and W-1, for the elements Cu and Zn. From Table 1 the Compton line for RhK α line yields 2,327,864 counts for AGV-1 and 2,110,546 counts for W-1. Using Figure 4, mass absorption coefficients of 4.14 and 5.05 $^\circ$ are obtained for AGV-1 and W-1 for the RhK α line. Using these values and Figure 5, the values of 56.63 and 69.25 for the μ CuK α for AGV-1 and W-1 are obtained. Using the same values and Figure 6, the values of 46.55 and 56.97 are

obtained for μ ZnK α for AGV-1 and W-1. The absolute values of the mass absorption coefficients obtained by various methods are not important as long as the ratio of the mass absorption coefficients is constant. The μ values are used to obtain the "apparent concentrations" from the standard formula for X-ray trace analysis of rocks (Hower, 1958; Reynolds, 1963):

$$C_{un} = C_{st} \times \frac{I_{un}}{I_{st}} \times \frac{\mu_{un}}{\mu_{st}}$$

where:

C = concentration,
I = intensity,
st = standard,
un = unknown, and
 μ = mass absorption coefficient.

From Table 6, the ratio of values, regardless of the method, can be deduced to be very close to 0.82 $^\circ$.

Once the mass absorption coefficient of the rock or soils is obtained for the particular element, which also is a target contaminant giving interfering intensities, then graphs plotting intensity (counts) of interfering spectral lines from the target versus the mass absorption coefficient of the element are used. Such graphs are presented in figures 1, 2, and 3.

Table 5 shows that the AGV-1 sample has a μ CuK α value of 56.63, and Figure 1 yields an interference value of 42,363 counts. By subtracting this value from the total intensity of 47,689 counts a value of 5,326 counts is obtained. Similarly, for W-1, a net count of 8,114 is obtained. Thus,

$$C_{Cu} = 59 \times \frac{8114}{5326} \times \frac{69.25}{56.63} = 110 \text{ ppm of Cu in W-1}$$

Similarly, the Zn concentration in W-1 is calculated as 87 ppm (Table 5).

Discussion

The results obtained by the two other methods for Cu, Zn and Pb are compared in Table 6 with the results derived from the technique described in this paper. The per cent variation between the three methods is acceptable since all values are based on the "accuracy" of the "usable values" (Abbey, 1980).

Steele's approach, as shown in the appendix, yields results which are very close to the ones presented in this work. However, Steele's method is relatively tedious for routine analysis of geological samples, when compared to the method proposed herein.

The results of the Pb determination show substantial discrepancies between the values obtained by the three different methods and the reported "usable value" (Abbey, 1980). The discrepancies are due either to counting errors originating from the coexistence of the K α arsenic line with the L α lead line, or to the fact that the reported "usable value" is incorrect. It would be more appropriate to use the L β line for Pb. However, the results obtained by the techniques used in this paper are very close to those obtained by Steele's method, so the techniques are not only faster but equally accurate.

¹Compton, A.H. and Allison, S.K. (1935).

The intensity of interfering lines from targets can also be approximately evaluated by an alternative method based on the following equation (Steele, 1973):

$$\delta I_{\lambda 1} = I_{\lambda 1}^{\text{ref}} \times I_{\lambda 2}^{\text{sample}} / I_{\lambda 2}^{\text{reference}}$$

where

$\delta I_{\lambda 1}$ = net interference intensity of the interfering spectral line for an element from the target in the unknown sample.

$I_{\lambda 1}^{\text{ref}}$ = net intensity of the interfering spectral line for an element from the target where the reference sample is free of that element.

$I_{\lambda 2}^{\text{sample}}$ = intensity of another spectral line from the tube, e.g. RhK α Compton line of the unknown sample.

$I_{\lambda 2}^{\text{reference}}$ = intensity of the spectral line from the tube, e.g. RhK α Compton line of the reference sample.

Using pure SiO₂ as a reference material, the intensity of the Cu interfering spectral line from the target is measured at 18,375 counts. Combining this value with the intensity of the RhK α Compton line from Table 6, the following is obtained:

$$\delta I_{\text{Cu AGV-1}} = 18,375 \times \frac{2,327,860}{2,859,111} = 14,960$$

This value compared with the value of 13,247 counts obtained from the use of S_{coh} factors (see Appendix) yields an 11.45 per cent (14,960-13,247)/14,960 variation. This variation is similar to the one predicated by Steele (1973). It seems that this alternative method is a good approximation because it requires less work than any of the other methods. However, it is the feeling of both authors that errors can be compounded if approximate methods such as this alternative method become a routine part of chemical analysis.

References

- Abbey, S.
1980: Studies in "standard samples" for use in the general analysis of silicate rocks and minerals; Geological Survey of Canada, Paper 80-14.
- Compton, A.H. and Allison, S.K.
1935: X-rays in theory and experiment; Van Nostrand, New York, New York, 2nd edition, 828 p.
- Cromer, D.T. and Waber, J.T.
1965: Scattering factors computed from relativistic Dirac-Slater wave function; Acta Crystallographica, v. 18, p. 104-109.
- Flanagan, F.J.
1969: U.S. Geological Survey standards. First compilation of data for the new U.S.G.S. rocks; Geochimica Cosmochimica Acta, v. 33, p. 81-131.
- Franzini, M., Leoni, L., and Saitta, M.
1976: Determination of the X-ray mass absorption coefficient by measurement of the intensity of Ag K α Compton scattered radiation; X-ray Spectrometry, v. 5, p. 84-87.
- Hower, T.
1959: Matrix corrections in the X-ray spectrographic trace-element analysis of rocks and minerals; American Mineralogist, v. 44, p. 19-32.
- Jenkins, R. and De Vries, J.L.
1969: Practical X-ray Spectrometry; Springer-Verlag, New York, New York, 2nd edition, 190 p.
- Reynolds, R.C., Jr.
1963: Matrix corrections in trace-element analysis by X-ray fluorescence: estimation of the mass absorption coefficient by Compton scattering; American Mineralogist, v. 48, p. 1133-1143.
1967: Estimation of mass absorption coefficients by Compton scattering: improvement and extensions of the method; American Mineralogist, v. 52, p. 1493-1502.
- Schöll, E. and Stepán, E.
1969: Zur röntgenfluoreszenz analyse geologischer materials; Tschermaks Mineralogische und Petrographische Mitteilungen, v. 13, p. 131-147.
- Steele, W.K.
1973: The correction of X-ray fluorescence analysis for scattered background peaks of target elements; Chemical Geology, v. 11, p. 149-156.
- Sumartojo, J. and Paris, M.W.
1980: A method for measuring X-ray mass absorption coefficients of geological materials; Chemical Geology, v. 28, p. 341-347.

APPENDIX

Calculations for Cu and Zn concentrations in W-1 rock samples (given AGV-1 as the standard rock sample whose Cu and Zn concentrations are 59 and 110 ppm respectively)

According to Steele's approach, the theoretical expressions for calculating the interfering spectral lines from targets are based on the following two equations:

$$1. S_{\text{coh}} = \frac{\sum_i (C_i F_i^2) / A_i}{\sum_i C_i \mu_i}$$

and 2.

$$\delta I_{\lambda} = I_{\lambda}^{\text{ref}} \cdot (S_{\text{coh}\lambda}^{\text{sample}}) / (S_{\text{coh}\lambda}^{\text{ref}})$$

where

i = Element in question

S_{coh} = Coherent scattering

Σ = Summation factor

C_i = Weight fraction = concentration of a given element obtained from the chemical analysis

F = Atomic scattering factor, obtained from table for the take-off angle of a particular XRF unit, divided by the wavelength of the element under examination

A = Atomic weight of an element

μ = Mass absorption coefficient

I_{λ}^{ref} = Net intensity of the interfering spectral line in the reference sample which is free from this element

δI_{λ} = Net interference intensity of the element from the target to be measured in the unknown sample.

To make use of equation 2, a solution to equation 1 is necessary. Equation 1 is solved for Cu in Table 7 and equation 1 is solved for Zn in Table 8, using AGV-1 and W-1 standard rock samples as well as pure compounds of SiO₂, CaO, Al₂O₃ and Li₂B₄O₇.

The elemental composition for AGV-1 and W-1 as oxides is given by Abbey (1980):

Samples	Elements									Total
	SiO ₂	Al ₂ O ₃	Fe ₂ O ₃	TiO ₂	MnO	MgO	CaO	Na ₂ O	K ₂ O	
AGV-1	59.61	17.19	6.78	1.06	0.10	1.52	4.94	4.32	2.92	98.44
W-1	52.72	15.02	11.11	1.07	0.17	6.63	10.98	2.15	0.64	100.49

To obtain the intensity of the interfering spectral line for Cu, one pure compound is needed. In this example, pure SiO₂ has been used as a reference material. The CuK α intensity yielded 18,375 counts.

Using the S_{coh} values for AGV-1 and pure SiO₂ from Table 7, the following interfering intensity for Cu from the target (Rh tube) is obtained:

$$\delta I_{\text{Cu}}_{\text{AGV-1}} = 18,375 \times \frac{0.0279}{0.0387} = 13,247 \text{ counts}$$

The 28,612 background counts are added to this result and the total (41,859 counts) is subtracted from the total measured Cu intensity on AGV-1. The result is 47,689 counts (see Table 6).

Therefore, the net intensity for Cu in AGV-1 is:

$$47,689 - (28,612 + 13,247) = 5,830 \text{ counts}$$

Using the S_{coh} value for W-1 and pure SiO₂ from Table 7, the following interfering intensity of the target for Cu is obtained:

$$\delta I_{\text{Cu}}_{\text{W-1}} = 18,375 \times \frac{0.0248}{0.0387} = 11,775 \text{ counts}$$

The 25,930 background counts are added to this figure and the total is subtracted from the total measured intensity for Cu in W-1. The latter value is 46,792 counts.

Therefore, the net intensity for Cu in W-1 is:

$$46,792 - (25,930 + 11,775) = 9,087 \text{ counts}$$

The concentration of Cu in W-1 can be calculated using the known Cu concentration of 59 ppm for AGV-1 as follows:

$$C_{\text{un}} = C_{\text{st}} \times \frac{I_{\text{un}}}{I_{\text{st}}} \times \frac{\mu_{\text{un}}}{\mu_{\text{st}}} = 59 \times \frac{9087}{5830} \times \frac{66.43}{54.29} = 113 \text{ ppm of Cu}$$

The value of 113 ppm for W-1 is reported in Table 6.

Similarly, for Zn, the intensity for SiO₂ yields 7,546 counts. Using the S_{coh} values for AGV-1 and pure SiO₂ from Table 8, the following interfering intensity for Zn from the target (Rh tube) is obtained:

$$\delta I_{\text{Zn}}_{\text{AGV-1}} = 7,546 \times \frac{0.0368}{0.0509} = 5,456 \text{ counts}$$

The 23,637 background counts are added to the counts calculated, yielding a sum of 29,093. This sum is subtracted from the total measured Zn intensity for AGV-1, which is 36,326 counts.

Therefore, the net intensity for Zn in AGV-1 is:

$$36,326 - (23,637 + 5,465) = 7,233 \text{ counts}$$

Using the S_{coh} value for W-1 and pure SiO₂ from Table 8, the following interfering intensity for Zn from the target (Rh tube) is obtained:

$$\delta I_{\text{Zn}}_{\text{W-1}} = 7,546 \times \frac{0.0324}{0.0509} = 4,803 \text{ counts}$$

The 21,659 background counts are added to the count value calculated, yielding a sum of 26,462. This sum is subtracted from the total measured intensity for Zn in W-1, which is 32,727 counts.

Therefore, the net intensity for Zn in W-1 is:

$$32,727 - (21,659 + 4,803) = 6,265 \text{ counts}$$

The concentration of Zn in W-1 can be calculated using the known Zn concentration of 86 ppm for AGV-1 as follows:

$$C_{\text{un}} = C_{\text{st}} \times \frac{I_{\text{un}}}{I_{\text{st}}} \times \frac{\mu_{\text{un}}}{\mu_{\text{st}}} = 86 \times \frac{6265}{7233} \times \frac{54.99}{44.80} = 91 \text{ ppm of Zn}$$

The value of 91 ppm Zn for W-1 is reported in Table 6.

PART II
**COMPARISON OF X-RAY TUBES USED FOR MAJOR AND TRACE ELEMENT
ANALYSIS IN X-RAY FLUORESCENCE SPECTROSCOPY**

Abstract

A comparison study of the chromium (Cr), rhodium (Rh), molybdenum (Mo) and tungsten (W) tubes used in X-ray fluorescence spectroscopy, shows that the Rh tube provides the best overall performance on silicates, carbonates, soils and geologic materials.

Test results indicate that detection limits depend upon the tube used as well as the matrix in which the element is found. It is shown that, in some cases, the white radiation hump is the dominant influence, whereas, in other cases, tube characteristic lines are more important.

The Cr tube gives a lower detection limit and better sensitivity for elements with absorption edges longer than V (2.269Å), whereas the Rh, Mo and W tubes give lower detection limits and better sensitivities for elements with absorption edges shorter than V. The Rh tube is better than the Mo because molybdenum is a lighter element than rhodium. The Rh tube is also better than the W because of interference between the tungsten L lines and the K and L characteristic lines of elements being analyzed.

Résumé

Une étude comparative des tubes à chrome (Cr), à rhodium (Rh), à molybdène (Mo), et à tungstène (W), qui sont utilisées dans des procédés de spectrographie fluorescente à rayons, indique que la performance du tube à rhodium est généralement supérieure lorsqu'il s'agit des applications sur des échantillons siliceux, carbonatés, de sols et de matériaux géologiques.

Des résultats d'épreuves indiquent que des limites de détection sont liées aux tubes utilisées et à la matrice dans laquelle l'élément se trouve. On a constaté que dans certains cas, le maximum en radiation blanche a une influence dominante, toutefois, dans d'autres cas, les lignes caractéristiques du tube sont plus importantes.

Le tube à chrome donne une limite de détection inférieure et une sensibilité meilleure pour des éléments qui ont des marges d'absorption plus longues que V (2.269Å), tandis que des tubes à rhodium, à molybdène et à tungstène donnent des limites inférieures et des sensibilités supérieures pour des éléments qui ont des marges d'absorption plus courtes que V. Le tube de rhodium est supérieur à celui de molybdène parce que le molybdène est un élément plus léger que le rhodium. Le tube à rhodium est meilleur que celui à tungstène à cause de l'interférence entre les lignes L du tungstène et les lignes K et L caractéristiques des éléments analysés.

Introduction

In X-ray fluorescence spectroscopy a number of factors control the extent to which a particular element can be excited and thus analyzed. These include the following:

1. The primary spectrum and characteristic spectral lines of the X-ray tube.
2. Atomic number of the excitation anode.
3. Excitation wavelength relative to absorption edge of the element to be analyzed.
4. Acceleration voltage and tube current.

The usual source of excitation in X-ray fluorescence analysis is the energy defined as the primary spectrum of the excitation anode. Its intensity, which is a function of the anode composition determines how well the characteristic radiation will be excited in the specimen. The characteristic spectral lines of the X-ray tube can contribute a large part of the exciting radiation (Birks, 1969) if the X-ray tube has intense lines near the wavelength to be analyzed. For example, under optimum conditions, the L lines of tungsten (W) can contribute about 25 per cent and the K lines of chromium (Cr) about 75 per cent of the spectrum used for excitation.

Table 1
Operating Conditions

*kV	*mA	**Crystal	Collimator	Detector	Time	Condition	Elements
60	32	TlAP	CC	F	40 sec.	Vac.	Na, Mg, Al
60	32	TlAP	FC	F	40 sec.	Vac.	Si
60	32	Ge	CC	F	40 sec.	Vac.	P, S, Cl
60	32	LiF	FC	F	40 sec.	Vac.	K, Ca, Sc
60	32	LiF	CC	F+S	40 sec.	Vac.	Ti
40	16	LiF	FC	F+S	40 sec.	Vac.	V
60	32	LiF	FC	F+S	40 sec.	Vac.	Mn, Fe, Co, Ni, Cu, Zn, Ga, Ge, As, Br
40	60	LiF	FC	F+S	40 sec.	Vac.	Rb, Sr, Y, Zr, Nb
60	32	LiF	FC	F+S	40 sec.	Vac.	Tc, Ru, Ag, Cd, In, Sn, Sb

*kV and mA were partly chosen on the basis of the concentration of the element in the sample measured.

**Crystal was chosen due to its reflectivity and its analytical range.

The higher the atomic number of the anode material the more intense the continuum (Bertin, 1970), but the only effective part of the primary spectrum is the part which is of shorter wavelength than the absorption edge, λ_{abs} , of the element to be excited. However, within this interval of shorter wavelength, the continuum spectrum nearest the wavelength to be measured is the most effective. Target material and voltage determine the intensity in the effective part of the spectrum (Birks, 1969). The accelerating voltage (kV) can be used to enhance the spectral line relative to the background, whereas tube current (mA) is used to enhance the intensity of both the characteristic line and the background in a linear manner (Bertin, 1970).

In this study an attempt has been made to evaluate various tubes under given operating conditions and to determine which tube is the most efficient for the excitation of elements in silicate, soil, coal ash and carbonate analysis. It will be shown that the rhodium (Rh) tube is acceptable for the entire range of elements to be analyzed, both for major and trace elements.

Materials and methods

Various mixtures of elements were prepared as oxides, metals, fused beads or pressed rock powders and made into discs. Intensity responses (counts per second) for the elements from Na (lightest) to Sb (heaviest) were measured on the K_{α} line.

For every element, counts on each disc were allowed to accumulate for 40 seconds. The counts obtained on the Cr tube for each element were used as the reference. The reference count for each element was divided into the count obtained for that element on each of the other tubes in order to obtain the relative responses.

Predetermined voltage and current were selected for each run. These and other operating conditions are summarized in Table 1. All or part of the white radiation plus tube spectral lines contributed to the excitation of the elements, depending on the wavelength to be excited.

All the samples were run on a Philips' Sequential Spectrometer, PW1212, under vacuum, using P10 (a mixture of 10% methane and 90% argon) as a carrier gas. Flux used in making glass beads was 5.0 g lithium tetraborate, 0.3 g lithium fluoride, and 1.0 g of ammonium nitrate. This mixture, along with the sample, was heated and fused on a Claisse Fluxer at 1000°C. Cellulose acetate was used as a binder in the pressed disc.

Results

The detector responses were normalized to those obtained with the Cr tube and plotted (figs. 1-3). The Rh tube gave reduced values (down to 0.5) for elements of atomic numbers $Z = 11$ to 16, and a further gradual decrease from 0.5 to about 0.2 for atomic numbers $Z = 16$ to 22 (Fig. 1). Results for the molybdenum (Mo) and tungsten (W) tubes give even lower values. There is a fairly constant relative intensity of about 0.2 for Mo and 0.3 for W for the region of atomic numbers $Z = 11$ to 22 (figs. 2, 3). Sharp increases in relative intensity occur for the Rh, Mo, and W tubes in the region of atomic numbers $Z = 23$ to 25, followed by more gradual increases (figs. 1-3). The Rh tube response peaks at atomic number $Z = 43$ and then drops suddenly, levelling out at about double the intensity of the Cr tube (Fig. 1). The Mo tube is very similar, except that it peaks at atomic number $Z = 39$, dropping suddenly afterward and levelling out at 1.5 (Fig. 2). The W tube has similar characteristics, except the peak occurs at atomic number $Z = 28$, dropping suddenly and then showing a gradual increase from 3 to 3.7 (Fig. 3).

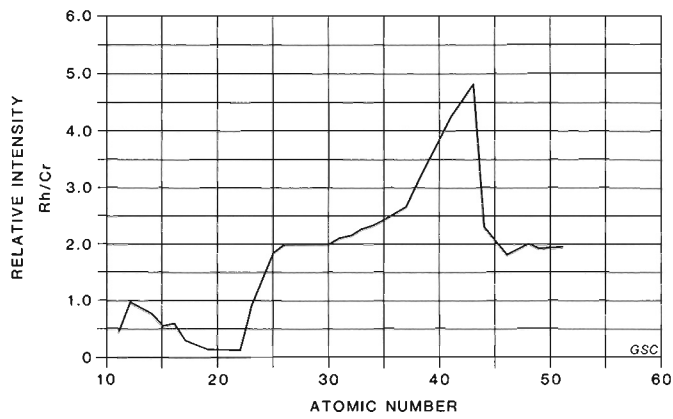


Figure 1. Relative intensity of Rh/Cr vs. atomic number.

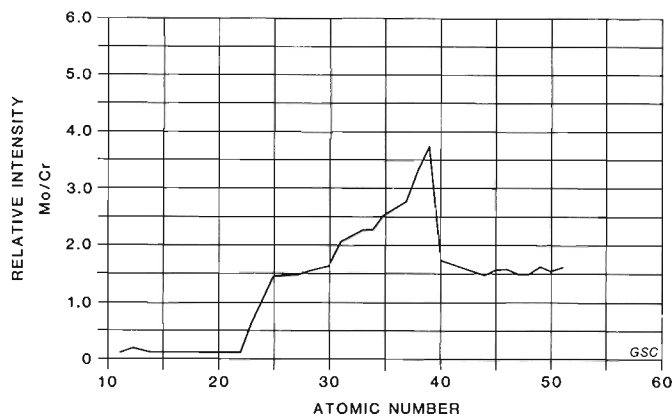


Figure 2. Relative intensity of Mo/Cr vs. atomic number.

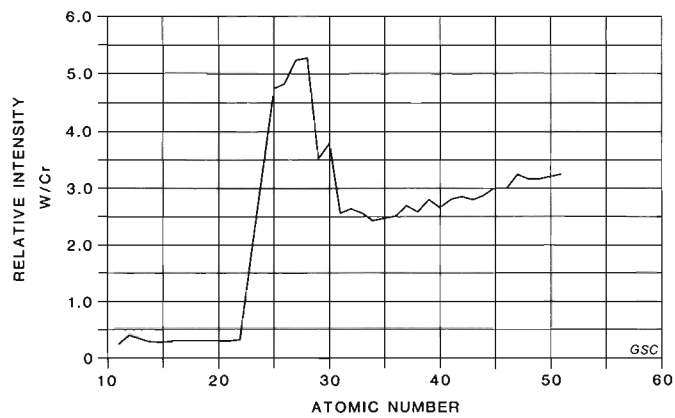


Figure 3. Relative intensity of W/Cr vs. atomic number.

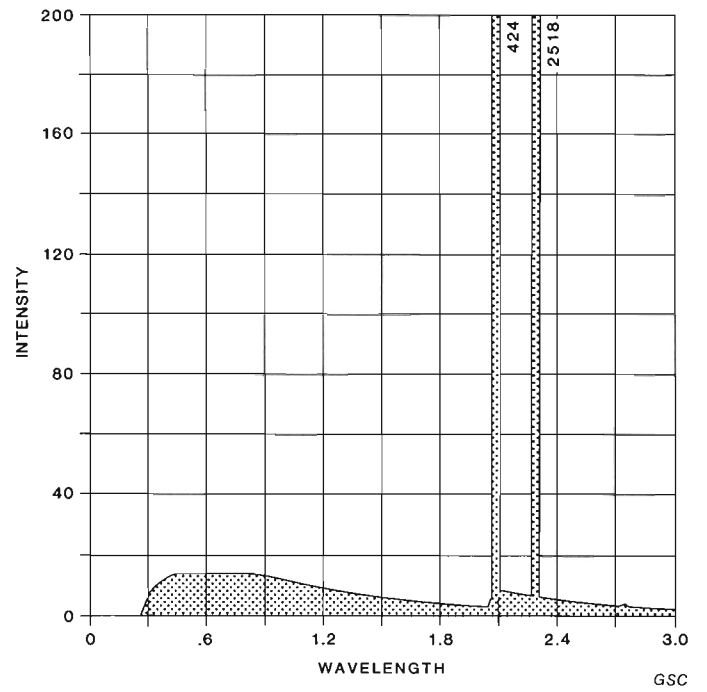


Figure 4. Spectrum intensity of Cr vs. wavelength.

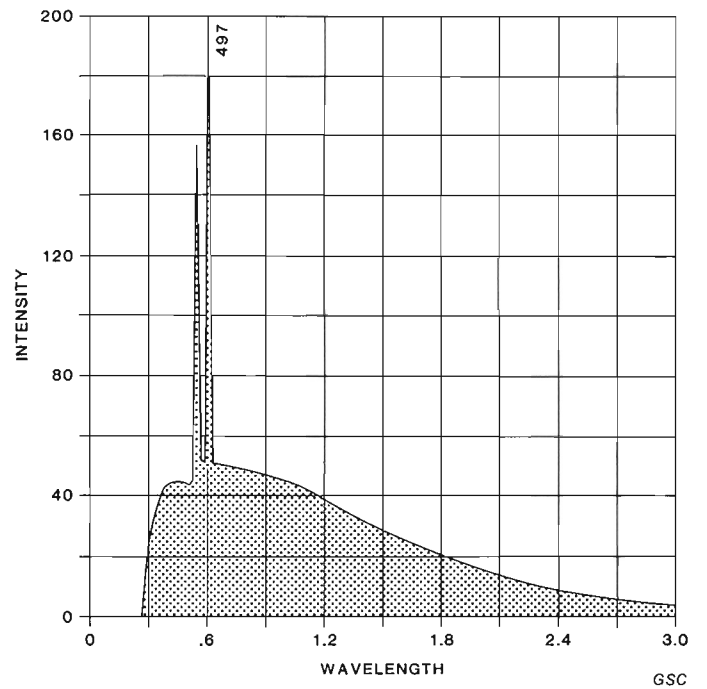


Figure 5. Spectrum intensity of Rh vs. wavelength.

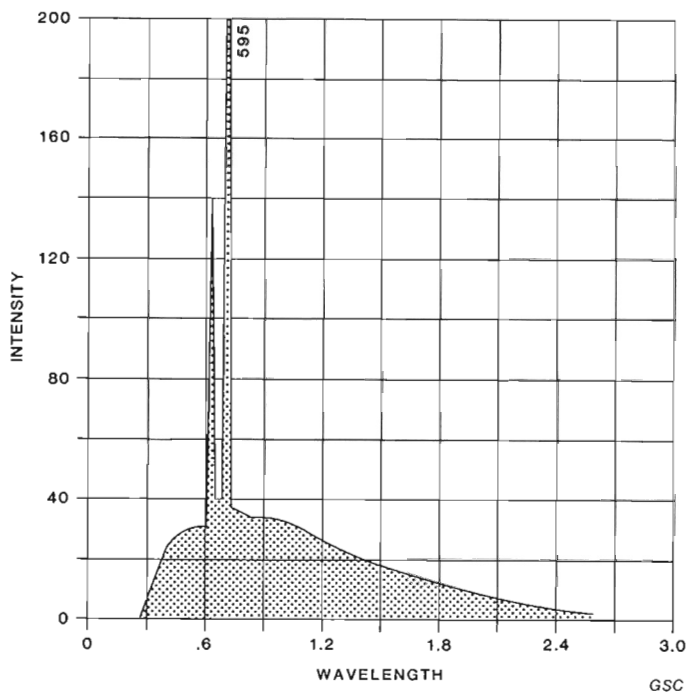


Figure 6. Spectrum intensity of Mo vs. wavelength.

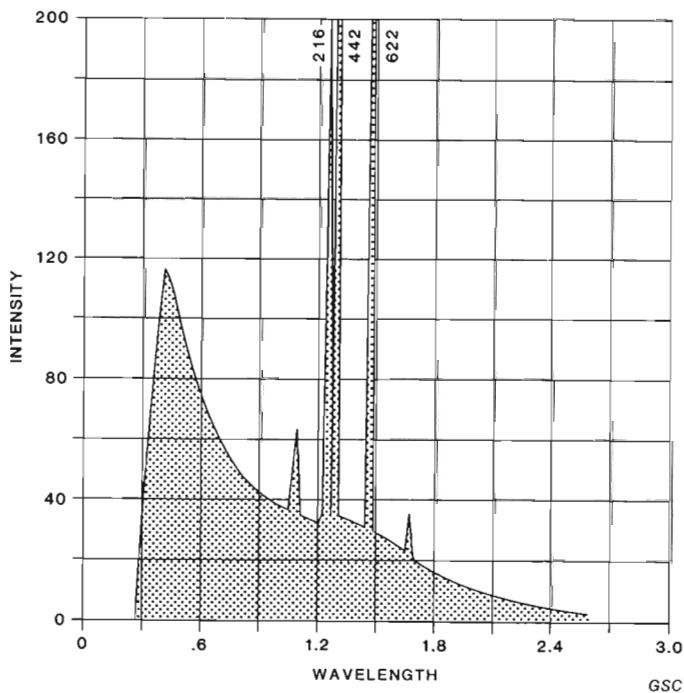


Figure 7. Spectrum intensity of W vs. wavelength.

Discussion

Figures 1, 2 and 3 indicate that the Cr tube gives more net intensity (cps) than the Rh, Mo or W tubes, for elements with wavelengths longer than the absorption edge of V ($2,269\text{\AA}$). For heavier elements, the detection limit is lower for the Cr tube than for any other (Table 2). Detection limits for Na through Si on the Rh tube are lower, by a factor of 3, than those for the Cr tube. For elements with absorption edges less than V, the Rh, Mo and W tubes give higher net intensities and, as a result, lower detection limits (Table 2).

The white radiation of the W tube is more effective for excitation than the white radiation of each of the other three tubes. However, Cr can be most useful for light elements ($Z \leq 22$) because its spectral lines contribute greatly in the excitation of these elements (figs. 4, 5, 6, 7). The spectral lines for Cr occur at a long wavelength (Cr $K_{\alpha} = 2.29\text{\AA}$) so that the Rh or Mo tubes are more effective for all elements with short wavelengths. The W tube is less useful because of the direct interference between its lines and the characteristic K or L lines of the various elements being analyzed. Table 3 summarizes the useful ranges of the various tubes.

The effect of tube voltage on the primary spectral distribution in a Rh target tube, and the corresponding effect on the intensity of the characteristic line of a Sr specimen, are shown in Figure 8. As the area of white radiation and tube spectral lines to the left (short wavelength) side of the Sr absorption edge increases, so does the net intensity of the K lines for Sr. It is shown that a voltage of 15 kV is insufficient to excite any Sr lines; the critical voltage being 16.2 kV. As the voltage is raised, the available radiation for excitation is increased (Fig. 8). Voltage, in part, determines the intensity of the effective part of the spectrum. Figures 4, 5, 6, and 7 show how the tube spectra of Cr, Rh, Mo and W compare, when analyzed at 45 kV (Birks, 1970).

Conclusion

The Cr tube is the superior tube for analysis of light elements with an atomic number $Z \leq 22$. In theory, the W tube is the best tube for elements with an atomic number $Z \geq 22$. However, because of spectral line interferences, W is preferred in certain instances only. For analysis of a wide range of elements, the Rh tube is the most adaptable and can be used effectively for major and trace element analysis in rocks, soils, coal ashes and carbonates.

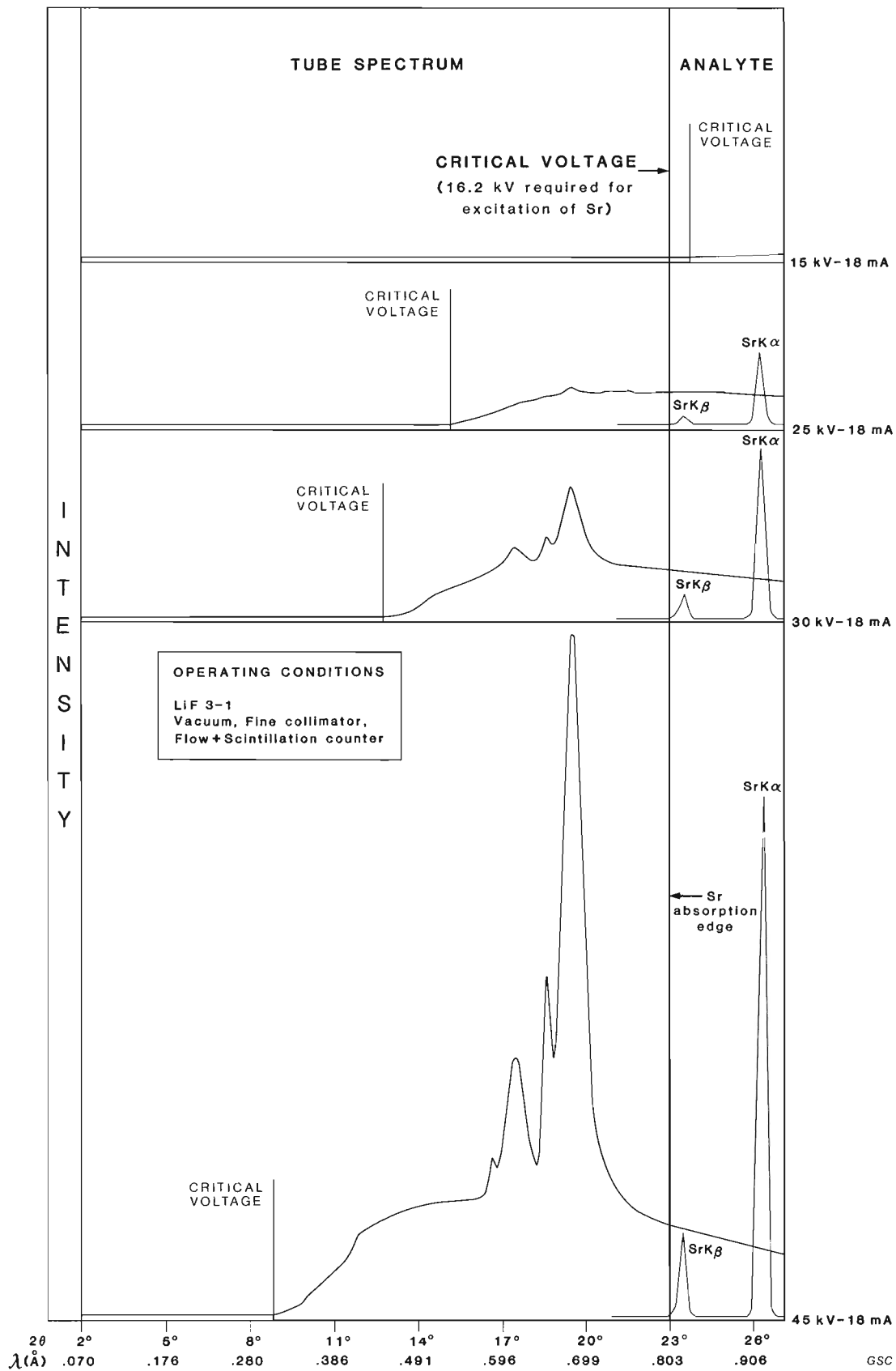


Figure 8. Illustration of tube spectrum and analyte spectrum.

Table 2

Comparison of detection limits

Ratio of LLDS	Na	Si	P	K	Ca	Ti	V	Mn	Fe	Co	Ni	Zn	As	Rb	Sr	Ru	In	Sn	Sb
$\frac{LLD\ Rh}{LLD\ Cr}$	2.33	1.46	3.42	2.82	6.41	7.25	1.13	.59	.74	.70	.71	.68	.67	.55	.41	.66	.76	.77	.81
$\frac{LLD\ Mo}{LLD\ Cr}$	10.95	10.12	18.07	5.86	3.74	8.19	1.16	.65	1.04	.80	.70	.60	.52	.45	.33	.71	.61	.80	.91
$\frac{LLD\ W}{LLD\ Cr}$	4.72	4.01	4.72	4.56	2.09	3.74	.83	.40	.36	.50	.55	.50	.64	.48	.64	.51	.45	.62	.57

Table 3

Optimum tubes for elements analyzed

	Na	Si	P	K	Ca	Ti	V	Mn	Fe	Co	Ni	Zn	As	Rb	Sr	Ru	In	Sn	Sb
Cr Tube	Best tube						E q u a l	Worst tube											
Rh Tube	Better than Mo and W			Worst tube	Better than Mo			Slightly better than Mo	E q u a l	Slightly worse than Mo						Slightly better than Mo			
Mo Tube	Worst tube			Better than Rh		Worst tube		Slightly worse than Rh		Slightly better than Rh						Slightly worse than Rh			
W Tube	Better than Mo			Better than Rh or Mo				W Slightly better	In some cases this tube is slightly better than Rh and Mo, except for the influence of tungsten L lines										
								Rh, Mo and W tubes are fairly close to equal											

GSC

References

Birks, L.S.
1969: X-ray spectrochemical analysis; Chemical Analysis, v. II, Interscience Publishers, 137 p.

Bertin, E.P.
1970: Principles and practice of X-ray spectrometric analysis; Plenum Press, New York, 671 p.

Acknowledgments

Professor J. Nicholls, Department of Geology, University of Calgary, D.W. Morrow of the Geological Survey of Canada, and C. Whitelaw of Philips Electronics, Toronto, are thanked for their reviews of both parts of this paper.